

## Dispersions of Individual Single-Walled Carbon Nanotubes of High Length

J. I. Paredes\* and M. Burghard

Max-Planck-Institut fuer Festkoerperforschung,  
Heisenbergstrasse 1, D-70569 Stuttgart, Germany

Received January 19, 2004. In Final Form: April 1, 2004

### Introduction

Owing to their unique physical and chemical properties,<sup>1,2</sup> carbon nanotubes and particularly single-walled carbon nanotubes (SWCNTs) are very promising for a wide range of applications, for example, as components of nanoelectronic devices (field-effect transistors, interconnects, etc.), as mechanically reinforced composite materials, or as miniaturized chemical sensors.<sup>3</sup> However, the realization of many of the proposed applications is hampered by several difficulties encountered in the processing and manipulation of the nanotubes. One of the major hurdles is the inherent insolubility of the tubes in common organic solvents and water.<sup>4</sup> Various strategies have been followed to achieve solubilization of SWCNTs that rely upon functionalization of the nanotube side wall or open ends to create an appropriate interface between the SWCNTs and the solvent.<sup>5–8</sup> Both covalent<sup>5–14</sup> and noncovalent<sup>5,15–25</sup> functionalization methods have been

explored toward this end. However, because the former methods often lead to at least partial degradation of the physical and electronic structure of the nanotubes, the noncovalent approaches appear more attractive because they enable the preservation of the nanotube's intrinsic properties.<sup>26</sup>

Despite the successful achievement of nanotube dissolution, most of the methods reported to date result in only partial exfoliation of the SWCNT ropes so that the tubes are dispersed as more or less thin bundles rather than as fully isolated individual objects. Although crucial for many applications,<sup>27–31</sup> the issue of disentangling the SWCNT ropes into individually dispersed tubes in bulk quantities essentially free of bundles has only very recently been solved.<sup>15,16,23,32</sup> In this respect, a major current problem lies in the fact that the tubes in these individual dispersions are shortened to lengths between 80 and 200 nm<sup>15,16,23,32</sup> as a result of the rather harsh conditions employed for dispersion. Although dispersions of such short individual SWCNTs are useful for certain aspects of nanotube science,<sup>33,34</sup> this length is too small for many practical applications. For instance, in nanotube-based electronics the separation of nanotubes according to their electronic type, which requires the use of bundle-free dispersions of individual SWCNTs, is a crucial problem that is only now being solved.<sup>28</sup> The separation would allow in principle the fabrication of, for example, thin film transistors consisting of purely semiconducting SWCNT networks,<sup>35</sup> but tubes with lengths exceeding  $\sim 1 \mu\text{m}$  would be highly preferable for that purpose. Likewise, for nanotube-reinforced composites, full-length individual tubes are also much more advantageous than short or bundled ones because the former allow for a better reinforcing effect.<sup>11,36</sup> It is then clear that having dispersions of individual SWCNTs of high length would be beneficial for these purposes.

Here, we report a straightforward procedure to prepare aqueous dispersions consisting of long, individual SWCNTs. The key feature of this method is a sequence of different types of mild ultrasonic treatments, which minimizes tube shortening and allows maximal preserva-

\* Corresponding author. Telephone number: (+49) 711 689 1346. Fax number: (+49) 711 689 1010. E-mail address: j.paredes@fkf.mpg.de.

- (1) Ajayan, P. M. *Chem. Rev.* **1999**, *99*, 1787–1799.
- (2) Dresselhaus, M. S.; Dresselhaus, G.; Avouris, Ph., Eds. *Carbon Nanotubes: Synthesis, Structure, Properties, and Applications*; Springer: Berlin, 2001.
- (3) Baughman, R. H.; Zakhidov, A. A.; de Heer, W. A. *Science* **2002**, *297*, 787–792.
- (4) Niyogi, S.; Hamon, M. A.; Hu, H.; Zhao, B.; Bhowmik, P.; Sen, R.; Itkis, M. E.; Haddon, R. C. *Acc. Chem. Res.* **2002**, *35*, 1105–1113.
- (5) Hirsch, A. *Angew. Chem., Int. Ed.* **2002**, *41*, 1853–1859.
- (6) Bahr, J. L.; Tour, J. M. *J. Mater. Chem.* **2002**, *12*, 1952–1958.
- (7) Sun, Y.-P.; Fu, K.; Lin, Y.; Huang, W. *Acc. Chem. Res.* **2002**, *35*, 1096–1104.
- (8) Banerjee, S.; Kahn, M. G. C.; Wong, S. S. *Chem. Eur. J.* **2003**, *9*, 1898–1908.
- (9) Khabashesku, V. N.; Billups, W. E.; Margrave, J. L. *Acc. Chem. Res.* **2002**, *35*, 1087–1095.
- (10) Holzinger, M.; Abraham, J.; Whelan, P.; Graupner, R.; Ley, L.; Hennrich, F.; Kappes, M.; Hirsch, A. *J. Am. Chem. Soc.* **2003**, *125*, 8566–8580.
- (11) Viswanathan, G.; Chakrapani, N.; Yang, Y.; Wei, B.; Chung, H.; Cho, K.; Ryu, C. Y.; Ajayan, P. M. *J. Am. Chem. Soc.* **2003**, *125*, 9258–9259.
- (12) Sano, M.; Kamino, A.; Okamura, J.; Shinkai, S. *Langmuir* **2001**, *17*, 5125–5128.
- (13) Pompeo, F.; Resasco, D. E. *Nano Lett.* **2002**, *2*, 369–373.
- (14) Huang, W.; Fernando, S.; Lin, Y.; Zhou, B.; Allard, L. F.; Sun, Y.-P. *Langmuir* **2003**, *19*, 7084–7088.
- (15) O'Connell, M. J.; Bachilo, S. M.; Huffman, C. B.; Moore, V. C.; Strano, M. S.; Haroz, E. H.; Rialon, K. L.; Boul, P. J.; Noon, W. H.; Kittrell, C.; Ma, J.; Hauge, R. H.; Weisman, R. B.; Smalley, R. E. *Science* **2002**, *297*, 593–596.
- (16) Islam, M. F.; Rojas, E.; Bergey, D. M.; Johnson, A. T.; Yodh, A. G. *Nano Lett.* **2003**, *3*, 269–273.
- (17) Schaefer, D. W.; Zhao, J.; Brown, J. M.; Anderson, D. P.; Tomlin, D. W. *Chem. Phys. Lett.* **2003**, *375*, 369–375.
- (18) Chen, J.; Liu, H.; Weimer, W. A.; Halls, M. D.; Waldeck, D. H.; Walker, G. C. *J. Am. Chem. Soc.* **2002**, *124*, 9034–9035.
- (19) Star, A.; Stoddart, J. F. *Macromolecules* **2002**, *35*, 7516–7520.
- (20) Wang, J.; Musameh, M.; Lin, Y. *J. Am. Chem. Soc.* **2003**, *125*, 2408–2409.
- (21) Bandyopadhyaya, R.; Nativ-Roth, E.; Regev, O.; Yerushalmi-Rozen, R. *Nano Lett.* **2002**, *2*, 25–28.
- (22) Star, A.; Steuerma, D. W.; Heath, J. R.; Stoddart, J. F. *Angew. Chem., Int. Ed.* **2002**, *41*, 2508–2512.

(23) Zheng, M.; Jagota, A.; Semke, E. D.; Diner, B. A.; McLean, R. S.; Lustig, S. R.; Richardson, R. E.; Tassi, N. G. *Nat. Mater.* **2003**, *2*, 338–342.

(24) Sun, Y.; Wilson, S. R.; Schuster, D. I. *J. Am. Chem. Soc.* **2001**, *123*, 5348–5349.

(25) Choi, N.; Kimura, M.; Kataura, H.; Suzuki, S.; Achiba, Y.; Mizutani, W.; Tokumoto, H. *Jpn. J. Appl. Phys.* **2002**, *41*, 6264–6266.

(26) Richard, C.; Balavoine, F.; Schultz, P.; Ebbesen, T. W.; Mioskowski, C. *Science* **2003**, *300*, 775–778.

(27) Doorn, S. K.; Strano, M. S.; O'Connell, M. J.; Haroz, E. H.; Rialon, K. L.; Hauge, R. H.; Smalley, R. E. *J. Phys. Chem. B* **2003**, *107*, 6063–6069.

(28) Krupke, R.; Hennrich, F.; Löhneysen, H. v.; Kappes, M. M. *Science* **2003**, *301*, 344–347.

(29) Chen, Z.; Du, X.; Du, M.-H.; Rancken, C. D.; Cheng, H.-P.; Rinzler, A. G. *Nano Lett.* **2003**, *3*, 1245–1249.

(30) Ajayan, P. M.; Schadler, L. S.; Giannaris, C.; Rubio, A. *Adv. Mater.* **2000**, *12*, 750–753.

(31) Dyke, C. A.; Tour, J. M. *Nano Lett.* **2003**, *3*, 1215–1218.

(32) Kovtyukhova, N. I.; Mallouk, T. E.; Pan, L.; Dickey, E. C. *J. Am. Chem. Soc.* **2003**, *125*, 9761–9769.

(33) Bachilo, S. M.; Strano, M. S.; Kittrell, C.; Hauge, R. H.; Smalley, R. E.; Weisman, R. B. *Science* **2002**, *298*, 2361–2366.

(34) Hartschuh, A.; Pedrosa, H. N.; Novotny, L.; Krauss, T. D. *Science* **2003**, *301*, 1354–1356.

(35) Snow, E. S.; Novak, J. P.; Campbell, P. M.; Park, D. *Appl. Phys. Lett.* **2003**, *82*, 2145–2147.

(36) Chen, J.; Rao, A. M.; Lyuksyutov, S.; Itkis, M. E.; Hamon, M. A.; Hu, H.; Cohn, R. W.; Eklund, P. C.; Colbert, D. T.; Smalley, R. E.; Haddon, R. C. *J. Phys. Chem. B* **2001**, *105*, 2525–2528.

tion of its structural and electronic properties. The degree of dispersion and length of the tubes were monitored by atomic force microscopy (AFM). Furthermore, optical absorption spectroscopy was used for a critical comparison between the electronic properties of individually dispersed as-produced and purified SWCNTs. This issue is of special relevance for all applications that sensitively depend on the density of defects in the nanotubes.

### Experimental Section

SWCNTs synthesized by the HiPco process,<sup>37</sup> both as-produced (batch CNI 002) and in purified form (batch CNI 26-0036B-2), were purchased from Carbon Nanotechnologies. In the experiments, the SWCNTs were dispersed in water by means of the surfactant sodium dodecylbenzene sulfonate (SDBS), which has recently been shown to allow the dispersion of the tubes as individuals in aqueous solution.<sup>16</sup> Nanotube dispersions were prepared by a combined tip and bath ultrasonication approach as follows. A small piece of HiPco SWCNT mat was added to an aqueous solution (5 mg/mL) of the surfactant and subjected to ultrasonic treatment in a tip sonicator (Dr. Hielscher UP 200s). A small number of pulses (usually five), with 0.5-s-on/0.5-s-off pulse cycles at  $\sim 40$  W/cm<sup>2</sup>, were applied to a volume of 1.5 mL. Subsequently, the obtained suspension was centrifuged (Eppendorf 5417C centrifuge) at 20 200g for 30 min. The upper  $\sim 80\%$  of the resulting supernatant was then carefully decanted and subjected to ultrasonication in a bath sonicator (Branson 1510, 80 kHz) for time periods ranging from a few minutes to several hours. For the characterization of the dispersed nanotubes by AFM, Si/SiO<sub>2</sub> substrates were first surface-modified with *N*-[3-(trimethoxysilyl)propyl]ethylenediamine. After immersion in the SWCNT dispersion for 15 min, the substrates were dried under a stream of nitrogen, thoroughly rinsed in ultrapure water, and dried again. AFM imaging was performed in the tapping mode with a Nanoscope Multimode IIIa microscope (Digital Instruments), employing commercial silicon cantilevers. UV-vis absorption spectra of the dispersions were acquired with a Lambda 2 spectrometer (Perkin-Elmer) in the range of 400–1100 nm.

### Results and Discussion

SWCNTs dispersed with the aid of the SDBS surfactant were characterized in detail at different stages of the procedure. After the first two steps, that is, tip sonication and centrifugation, the decanted supernatant was found to contain individual nanotubes and bundles with up to a 7-nm thickness (though predominantly thinner than 4 nm). About 50% of the objects were individual tubes (identified as features with heights below 1.3 nm in the AFM images),<sup>16</sup> whose lengths ranged from  $\sim 150$  nm to slightly above  $3 \mu\text{m}$ , with a mean value of  $820 (\pm 556)$  nm. By further treatment of the decanted supernatant in the low-power bath sonicator, the yield of individually dispersed tubes could be greatly improved. Most significantly, this additional step allowed the formation of relatively long dispersed tubes, provided that short sonication times ( $\leq 30$  min) were used. The AFM images of SWCNTs from a final dispersion prepared by a 30-min bath sonication, depicted in Figure 1, reveal the presence of mostly individual tubes. Different dispersions prepared under these conditions yielded about 80% isolated tubes, in agreement with earlier results attained with this surfactant.<sup>16</sup> It is also noticed that, in contrast to previous reports, the individual nanotubes are typically from several hundred nanometers to a few micrometers long. Figure 2 displays the length distribution of SWCNTs in this individual dispersion, as deduced from AFM measurements on  $\sim 400$  tubes. The average length of the

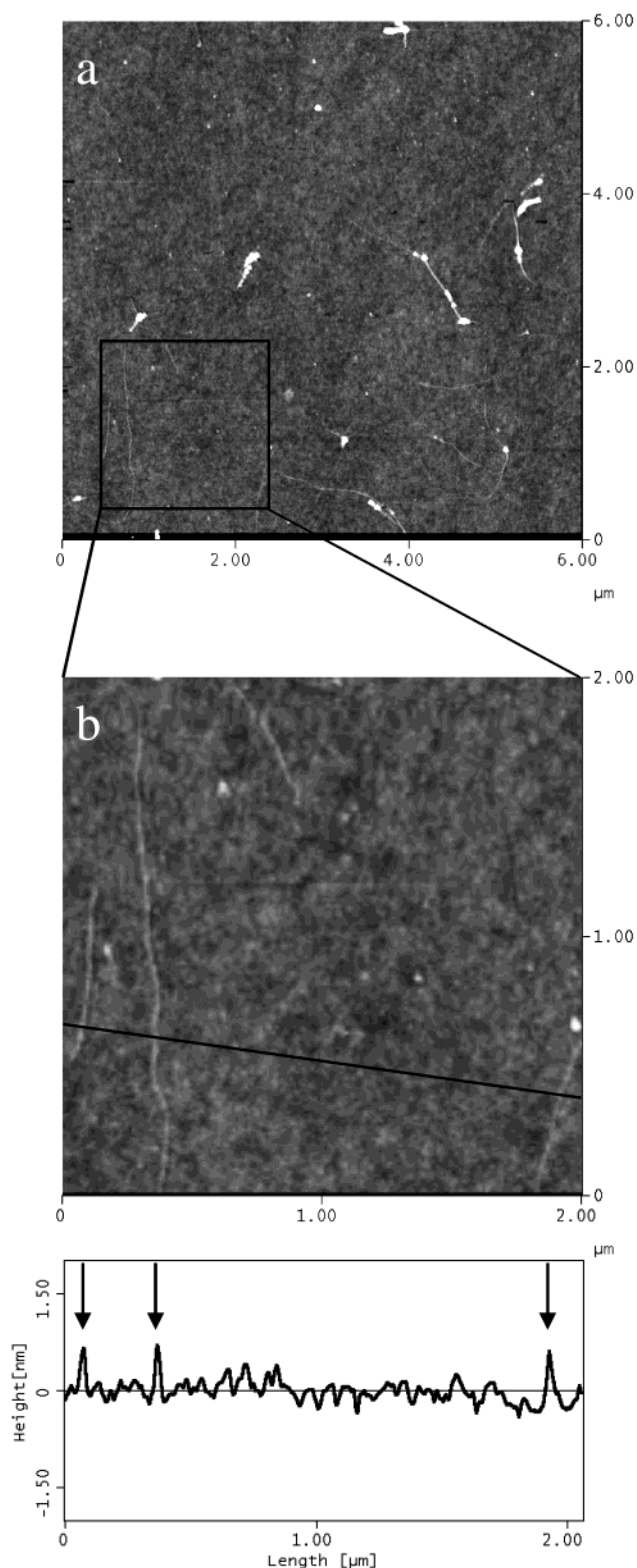


**Figure 1.** AFM images [(a) general view, (b) enlarged image of the square box in part a together with a height profile along the black line] of as-produced HiPco SWCNTs individually dispersed in water by means of SDBS and deposited onto a Si/SiO<sub>2</sub> substrate. The dispersion was prepared by a three-step procedure consisting of tip sonication (five pulses), centrifugation (30 min), and bath sonication (30 min). Z range for both images: 8 nm.

individual tubes was calculated to be  $770 (\pm 572)$  nm. This figure is 5–7 times larger than those recently documented for individually suspended HiPco tubes obtained with the same or similar surfactants.<sup>15,16</sup> Furthermore, in previous

(37) Chiang, I. W.; Brinson, B. E.; Huang, A. Y.; Willis, P. A.; Bronikowski, M. J.; Margrave, J. L.; Smalley, R. E.; Hauge, R. H. *J. Phys. Chem. B* **2001**, *105*, 8297–8301.

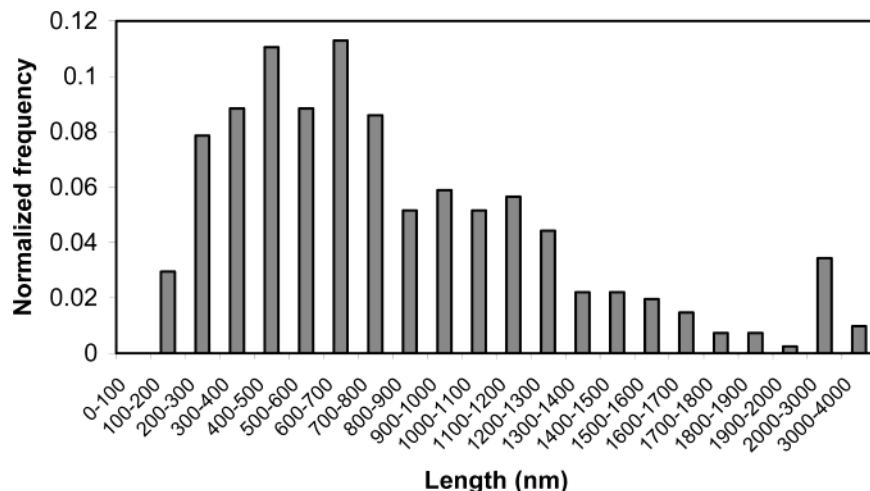


**Figure 2.** Length distribution histogram for the dispersion of individual nanotubes prepared by the same procedure as in Figure 1.

reports<sup>16</sup> virtually no HiPco tubes longer than 500 nm were observed in their individual dispersions, whereas in the present work comparable individual dispersions contain ~70% of tubes longer than 500 nm, and those longer than 1  $\mu\text{m}$  constitute ~30%. Dispersions of individual SWCNTs with these improved lengths should be particularly beneficial for the abovementioned applications in nanoelectronics and composites.<sup>11,35,36</sup> It is also worth noting that shorter bath sonication times (e.g., 10 min) did not lead to a significant increase in the yield of individually dispersed tubes, as compared with the starting dispersion (~50%), while considerably longer times resulted in a marked reduction of the nanotube lengths (e.g., no tubes longer than 1  $\mu\text{m}$  survived after a few to several hours of sonication). We believe that the gentle bath sonication (30 min) is effective in achieving a high yield of individually dispersed tubes while retaining their lengths, because it is applied to well-dispersed thin bundles, rather than to an entangled mat of thick bundles. In the latter case, very long sonication times would be required to individually disperse the tubes,<sup>16</sup> which would cause significant shortening.

To further support the observation that dispersions of individual SWCNTs basically free of bundles were obtained, we acquired UV-vis absorption spectra of such dispersions. It has been previously reported that such spectra are very sensitive to the aggregation state of nanotube suspensions.<sup>15</sup> Specifically, clear-cut differences were found between dispersions dominated by bundles and those dominated by individual tubes. Figure 3 shows the UV-vis absorption spectrum in the range 400–1100 nm of a SWCNT dispersion prepared by the same procedure as that used for the samples in Figures 1 and 2. The spectrum exhibits well-resolved features which arise from transitions between symmetrical van Hove (vH) singularities in the electronic density of states of the nanotubes. In the case of HiPco-produced SWCNTs, the absorption bands in the range of 400–600 nm originate from the first vH transitions of metallic tubes ( $M_{11}$ ), those within the 550–900 nm range correspond to the second vH transitions of semiconducting tubes ( $S_{22}$ ), and the bands within the 900–1100 nm range are due to first vH transitions ( $S_{11}$ ) of those semiconducting nanotubes in the dispersion with smaller diameters (the  $S_{11}$  transitions for the larger diameter semiconducting nanotubes in the dispersion lie at wavelengths above 1100 nm and up to 1600 nm).<sup>15</sup> The fact that well-defined absorption peaks in the 900–1100 nm range, as they are observed in Figure

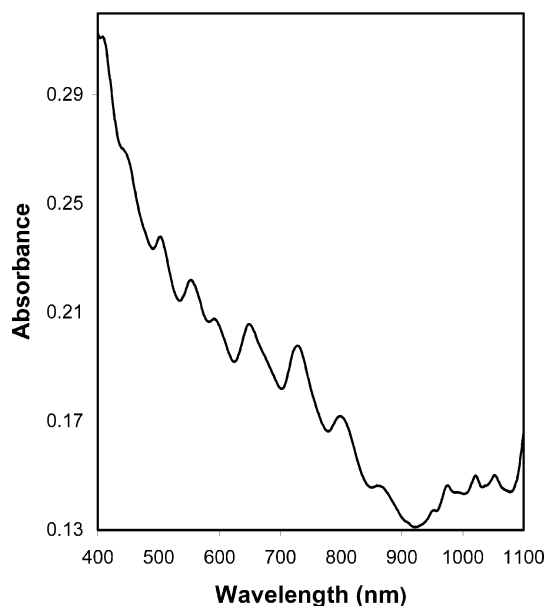


**Figure 3.** UV-vis absorption spectrum of as-produced HiPco SWCNTs individually dispersed in water by means of SDBS through the same procedure as in Figure 1.

3, can only be obtained for dispersions consisting essentially of individual (not bundled) tubes,<sup>15</sup> as well as the exact matching of the transition wavelengths ( $M_{11}$ ,  $S_{22}$ , and  $S_{11}$ ) of the spectrum of Figure 3 with those previously measured for pristine, surfactant- or DNA-coated individual HiPco tubes,<sup>15,23,38</sup> indicates the presence of nanotubes in our dispersions mostly in an intact, isolated state. Consequently, the AFM and UV-vis observations combined reveal that bundle-free dispersions of long, individual SWCNTs were successfully prepared. We should stress that if the dispersions were dominated by small nanotube bundles, rather than by individual tubes, no structure could be discerned in the  $S_{11}$  region between 900 and 1100 nm in the UV-vis spectra (i.e., no well-defined peaks would be present in this region), and the  $S_{22}$  and  $M_{11}$  peaks would appear broadened and red-shifted relative to those of Figure 3 because of intertube interactions within the bundles, as has been previously shown.<sup>15</sup> For this reason, we have used here the red shifting of the peaks in the UV-vis spectra as a highly sensitive indicator

(38) Moore, V. C.; Strano, M. S.; Haroz, E. H.; Hauge, R. H.; Smalley, R. E.; Schmidt, J.; Talmon, Y. *Nano Lett.* **2003**, *3*, 1379–1382.

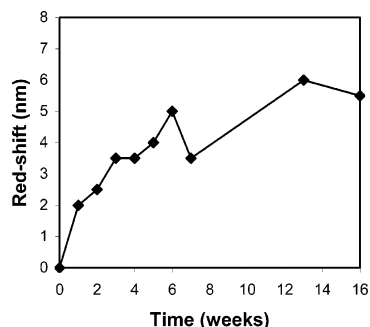


**Figure 4.** Plot for the red shift of the 800-nm peak in the spectrum of Figure 3 as a function of standing time of the dispersion.

to determine the rate of re-aggregation of the SWCNTs in our dispersions upon standing for long periods of time. For SDBS-stabilized dispersions of short, individual HiPco tubes, the preservation of visually homogeneous suspensions upon prolonged standing (e.g., 2 months) has been reported.<sup>16</sup> Although our suspensions of long, individual tubes also appeared homogeneous to the naked eye after similar periods of time, a red shift of the absorption features could be observed on the same time scale. As mentioned before, this shift is a sign of interactions between nanotubes and, consequently, of their re-aggregation into bundles. Figure 4 plots the red shift of the  $S_{22}$  peak located at  $\sim 800$  nm in the absorption spectrum of the individually dispersed nanotubes versus standing time. One observes a steady increase with time during the first weeks, followed by a plateau ( $\sim 5$ – $6$  nm or  $\sim 10$ – $12$  meV) after extended standing (16 weeks). The same trend with similar magnitudes of red shifting was noticed for peaks corresponding to  $S_{11}$  and  $M_{11}$  transitions. Because both the magnitude of the red shift is small compared to that measured for bundled HiPco tube dispersions ( $\sim 50$  meV)<sup>39</sup> and the  $S_{11}$  peaks remain largely unaltered (albeit broadened), we conclude that only limited rebundling occurs in the dispersions even after time periods of a few months.

Additionally, we compared the dispersion capability of the pristine, as-produced tubes with that of purified HiPco SWCNTs. As revealed by AFM, the latter type of tubes could be individually suspended in aqueous SDBS solution to the same extent (i.e., basically free of bundles) and with the same length distribution as the as-produced material. However, the UV–vis spectrum of the individual dispersions of purified HiPco tubes (Figure 5) was different from that of their as-produced counterparts (Figure 3). Although there is no complete loss of structure in the spectral features, implying that the purified tubes retain to some degree their original electronic structure, the  $M_{11}$  and  $S_{22}$  features appear significantly broadened, and the well-defined peaks in the  $\sim 900$ – $1100$  nm range characteristic of the individual dispersions of the as-produced tubes (Figure 3) are no longer present in the dispersions of the purified tubes. We do not attribute these spectral characteristics to a possible bundling of the purified SWCNTs because AFM revealed mostly individually isolated nanotubes in the same yields as those attained with as-produced tubes. Also, we rule out that protonation<sup>15</sup> of the purified tubes is responsible for the absence of well-defined transitions in the  $900$ – $1100$  nm range of the UV–vis spectrum (Figure 5) because the dispersions prepared with these tubes were only slightly acidic (pH

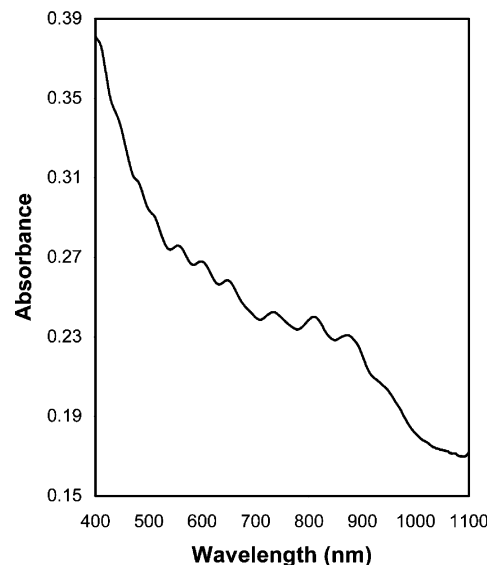


**Figure 5.** UV–vis absorption spectrum of purified HiPco SWCNTs individually dispersed in water by means of SDBS.

$\sim 5$ – $6$ ). Therefore, the differences between the spectra of Figures 3 and 5 should be directly attributed to changes induced by the purification process on the nanotube samples. The purification of HiPco SWCNTs usually involves oxidation,<sup>37</sup> which introduces oxygen functional groups and related defects onto the nanotubes.<sup>40</sup> Thus, the differences between the purified (Figure 5) and as-produced (Figure 3) nanotube samples could be possibly put down to oxidation effects during purification. As a matter of fact, bleaching of the  $S_{11}$  transitions has been previously reported for thin films of purified tubes and ascribed to the effects of purification by nitric acid.<sup>41</sup> These observations should be considered for evaluating the potential of purified, individually dispersed nanotubes for various applications.

## Summary

In summary, we have presented a suitable approach to obtain surfactant-stabilized suspensions of long, individually dispersed SWCNTs essentially free of bundles. The combination of mild tip and bath ultrasonication has proven effective in unbundling the SWCNT ropes and, at the same time, in minimizing tube shortening. This method is expected to be useful for applications that critically depend on the availability of bulk dispersions of long, individual tubes with minimized defect densities, such as for nanotube-based electronics and composite materials. Furthermore, the observed purification-induced changes in the electronic structure of HiPco SWCNTs indicate that care has to be taken when comparing their properties with those of the as-produced material.

**Acknowledgment.** J.I.P. acknowledges the Ministerio de Educación, Cultura y Deporte (Spain) for financial support. We also thank V. Skakalova (MPI Stuttgart) for helpful comments on the manuscript.

LA049831Z

(40) Du, W.-F.; Wilson, L.; Ripmeester, J.; Dutrisac, R.; Simard, B.; Dénomée, S. *Nano Lett.* **2002**, *2*, 343–346.

(41) Itkis, M. E.; Niyogi, S.; Meng, M. E.; Hamon, M. A.; Hu, H.; Haddon, R. C. *Nano Lett.* **2002**, *2*, 155–159.

(39) Hagen, A.; Hertel, T. *Nano Lett.* **2003**, *3*, 383–388.